Northumbria Research Link

Citation: Li, Jianquan, Dang, Nanmao, Martinez-Lopez, Nuria, Jowsey, Paul, Huang, Dong, Lightowlers, Robert N., Gao, Fei and Huang, Jun-Yong (2019) M2I-1 disrupts the in vivo interaction between CDC20 and MAD2 and increases the sensitivities of cancer cell lines to anti-mitotic drugs via MCL-1s. Cell Division, 14 (1). ISSN 1747-1028

Published by: BMC

URL: https://doi.org/10.1186/s13008-019-0049-5 <https://doi.org/10.1186/s13008-019-0049-5>

This version was downloaded from Northumbria Research Link: http://nrl.northumbria.ac.uk/43210/

Northumbria University has developed Northumbria Research Link (NRL) to enable users to access the University's research output. Copyright © and moral rights for items on NRL are retained by the individual author(s) and/or other copyright owners. Single copies of full items can be reproduced, displayed or performed, and given to third parties in any format or medium for personal research or study, educational, or not-for-profit purposes without prior permission or charge, provided the authors, title and full bibliographic details are given, as well as a hyperlink and/or URL to the original metadata page. The content must not be changed in any way. Full items must not be sold commercially in any format or medium without formal permission of the copyright holder. The full policy is available online: http://nrl.northumbria.ac.uk/policies.html

This document may differ from the final, published version of the research and has been made available online in accordance with publisher policies. To read and/or cite from the published version of the research, please visit the publisher's website (a subscription may be required.)

UniversityLibrary

Northumbria University
NEWCASTLE

Li et al. Cell Div (2019) 14:5
https://doi.org/10.1186/s13008-019-0049-5

Cell Division

RESEARCH Open Access

M2I-1 disrupts the in vivo interaction between CDC20 and MAD2 and increases the sensitivities of cancer cell lines to anti-mitotic drugs via MCL-1s

Jianquan Li[1,3], Nanmao Dang[1], Nuria Martinez-Lopez[1], Paul A. Jowsey[2], Dong Huang[1,4], Robert N. Lightowlers[1], Fei Gao[1] and Jun-Yong Huang[1*]

Abstract

Background: Drugs such as taxanes, epothilones, and vinca alkaloids are widely used in the treatment of breast, ovarian, and lung cancers but come with major side effects such as neuropathy and loss of neutrophils and as single agents have a lack of efficacy. M2I-1 (MAD2 inhibitor-1) has been shown to disrupt the CDC20-MAD2 interaction, and consequently, the assembly of the mitotic checkpoint complex (MCC).

Results: We report here that M2I-1 can significantly increase the sensitivity of several cancer cell lines to anti-mitotic drugs, with cell death occurring after a prolonged mitotic arrest. In the presence of nocodazole or taxol combined with M2I-1 cell death is triggered by the premature degradation of Cyclin B1, the perturbation of the microtubule network, and an increase in the level of the pro-apoptotic protein MCL-1s combined with a marginal increase in the level of NOXA. The elevated level of MCL-1s and the marginally increased NOXA antagonized the increased level of MCL-1, a pro-survival protein of the Bcl-2 family.

Conclusion: Our results provide some important molecular mechanisms for understanding the relationship between the mitotic checkpoint and programmed cell death and demonstrate that M2I-1 exhibits antitumor activity in the presence of current anti-mitotic drugs such as taxol and nocodazole and has the potential to be developed as an anticancer agent.

Keywords: M2I-1, Cyclin B1, MCL-1, Nocodazole, Taxol, Apoptosis

Background

The spindle assembly or mitotic checkpoint (SAC) monitors the microtubule and kinetochore attachments to prevent a premature metaphase to anaphase transition and therefore helps to maintain genomic stability [1–4]. The SAC can sense any unattached kinetochores and responds by producing diffusible signals which inhibit the activity of the anaphase-promoting complex or cyclosome (APC/C) [3]. The APC/C acts as an E3 ligase and is essential for ubiquitin-mediated degradation of target proteins [1, 4–6]. Cyclin B1 is an important substrate of the APC/C and plays a critical role in facilitating mitotic entry and exit by regulating Cdk1 kinase activity [7, 8]. The MCC (Mitotic checkpoint complex) is believed to be one of the most prominent SAC inhibitory signals and consists of four components, CDC20, MAD2, BUBR1, and BUB3 [5, 9, 10]. It is assembled from the two sub-complexes, CDC20-MAD2 and BUBR1-BUB3 [10, 11]. The evidence suggests that as well as forming during prometaphase and metaphase in response to unattached kinetochores, the CDC20-MAD2 sub-complex can also be formed in prophase before nuclear envelope breakdown [6, 12, 13]. This prophase associated and SAC

*Correspondence: junyong.huang@ncl.ac.uk
[1] Institute for Cell and Molecular Biosciences, Newcastle University, Framlington Place, Newcastle upon Tyne NE2 4HH, UK
Full list of author information is available at the end of the article

© The Author(s) 2019. This article is distributed under the terms of the Creative Commons Attribution 4.0 International License (http://creativecommons.org/licenses/by/4.0/), which permits unrestricted use, distribution, and reproduction in any medium, provided you give appropriate credit to the original author(s) and the source, provide a link to the Creative Commons license, and indicate if changes were made. The Creative Commons Public Domain Dedication waiver (http://creativecommons.org/publicdomain/zero/1.0/) applies to the data made available in this article, unless otherwise stated.

independent CDC20-MAD2 complex prevents the premature degradation of Cyclin B1 before the cell enters mitosis [6, 13].

Cells with depleted or down-regulated Cyclin B1 often undergo apoptosis [14, 15]. Many of the SAC components are essential, and abnormal up- or down-regulation of its activity often results in cells experiencing a prolonged mitotic arrest or prematurely exiting mitosis [3, 16]. This in turn might lead to tumorigenesis, but most of the cells will commit suicide by entering programmed cell death [17–19]. One consequence of this mitotic vulnerability has been the development of anti-mitotic drugs for cancer therapy [20–23]. In fact, traditional anti-mitotic drugs, such as taxanes, epothilones, and vinca alkaloids are widely used and have been proven to be successful in the clinical treatment of breast, ovarian, and lung cancers [24, 25]. However, because they target microtubules they lack specificity, which results in side effects such as peripheral neuropathy and rapid development of resistance, and as single agents they show a lack of efficacy [23, 26].

Blocking mitotic exit is an efficient way of inducing tumor cell death, so in principle, compounds that directly target the APC/C or MCC to cause cells to arrest in mitosis should be more efficacious and have no or fewer side effects. M2I-1 (MAD2 inhibitor-1) is the first small molecule that has been identified as an inhibitor of the CDC20-MAD2 interaction, which is an essential process in the assembly of the MCC and the inhibition of the APC/C [6, 27]. Here we report the discovery that M2I-1 enhances the sensitivity of cancer cell lines to anti-mitotic drugs which might be of use in antitumor therapy.

Results

M2I-1 promotes the sensitivity of cancer cell lines to anti-mitotic drugs

In HeLa cells a normal cell cycle lasts about 20 h with mitosis taking about 1 h [28], and the daughter cells then rapidly entering the next cell cycle. Nocodazole (NOC) is a microtubule poison, which causes depolymerisation of the microtubules and activation of the SAC to arrest the cell at prometaphase [29] and HeLa cells can tolerate treatment with 40–400 ng/ml nocodazole for up to 24 h with no significant DNA damage or cell death [30, 31], though, a prolonged mitotic arrest (> 24 h) can cause apoptosis [17, 29]. However, we have noticed that when HeLa cells were treated for 16 h with 60 ng/ml nocodazole combined with 50 μM M2I-1 (hereafter 'NOC + M2I-1'), there was a significant (16.4%) increase in cell death compared to cells treated with 60 ng/ml nocodazole or 50 μM M2I-1 alone (Fig. 1b). The dead cells were identified by their fragmented cell body, which in many cases looks like a typical apoptotic-body (Fig. 1a, asterisk) [32, 33].

There is no significant difference in the number of cell deaths seen in cells treated with 0.5% DMSO (control), and either 50 μM M2I-1 or 60 ng/ml nocodazole alone (Fig. 1b). There is no significant difference in the mitotic index between the DMSO control and M2I-1 treated cells and as expected, about 80% of cells were arrested in mitosis in response to nocodazole treatment (Fig. 1c). In contrast, however, cells treated with NOC + M2I-1 showed a significant (18.9%) reduction in the mitotic index compared to cells treated with nocodazole alone (Fig. 1c). This increase in cell death has also been observed in cells treated with Taxol combined with M2I-1 (Fig. 1d, e). To test if this is unique to HeLa cells, various apoptotic-sensitive cell lines, HT-29, A549, U2OS were examined under the same conditions. Results showed that treatment with NOC + M2I-1 increased the rate of cell death by a varying amount in all cases (Fig. 1f). Thus it appears that M2I-1 can potentiate the sensitivity of some cancer cells to anti-mitotic drugs like nocodazole and taxol.

The beginning of cell death occurred after prolonged mitotic arrest

Why M2I-1 in the presence of nocodazole should induce cell death is intriguing, as this contradicts what would be anticipated based on the original observations that M2I-1 disrupted the interaction between CDC20 and MAD2 and caused a weak SAC [6, 27]. We had anticipated that, at least initially, we would see less cell death

(See figure on next page.)

Fig. 1 M2I-1 promotes the sensitivity of cancer cell lines to anti-mitotic drugs. HeLa cells were treated with one of 0.5% DMSO, 50 μM M2I-1, 60 ng/ml nocodazole, or 60 ng/ml nocodazole + 50 μM M2I-1 in a 24-well plate for 16 h. Digital images of cells from three or four random areas of each well were taken using a digital camera mounted on a tissue culture microscope with a 20x objective lens and used to quantify the mitotic and apoptotic indices. **a** Sample images showing non-mitotic cells (arrows), normal mitotic cells (arrowheads), mitotically arrested cells (dash line arrows), and apoptotic cells (asterisk). **b**, **d** Apoptotic indices quantified from HeLa cells treated with 60 ng/ml (equivalent to 200 nM) nocodazole or 30 nM Taxol under different circumstances as indicated. **c**, **e** Mitotic indices quantified from HeLa cells treated with 60 ng/ml nocodazole or 30 nM Taxol under the circumstances indicated. **f** Apoptotic indices quantified from A549, HT-29 and U2OS cells under the same conditions as described above. All the quantitative data were produced from four independent experiments. n, total cell numbers used for quantification; Noc, nocodazole; M2I-1, MAD2 inhibitor-1. P value: *< 0.017; **< 0.001; ***< 0.0003; ****< 0.0001

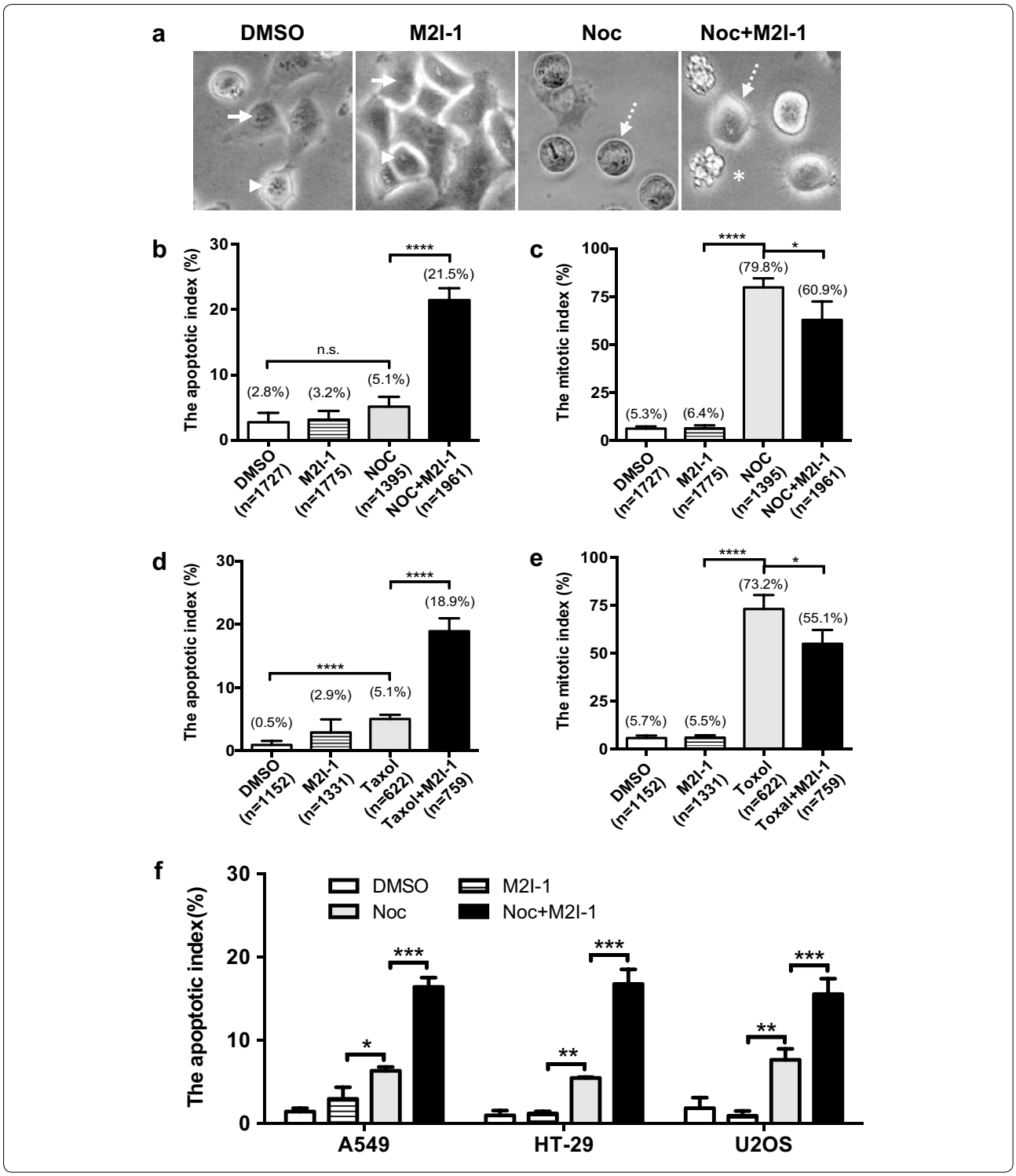

when the cells were treated with NOC + M2I-1 due to the weakened SAC leading to more slippage, and this was supported by the observations that there was a reduced mitotic index, and 15% lower level of histone H3 S-10 phosphorylation in samples treated with the NOC + M2I-1 compared to samples treated with nocodazole alone (Figs. 1c, 2a, b). As the observed cell death might be caused at some stage of the next cycle after

(See figure on next page.)

Fig. 2 The majority of cell deaths occurred after prolonged mitotic arrest. **a** Cell extracts were prepared from HeLa cells after 16 h of the different drug treatments as described previously. The western blot membranes were probed with a rabbit polyclonal anti-phospho-histone H3 (S-10) antibody (Millipore, #06-570) (1:500 dilutions), and the actin protein bands acted as the loading control. **b** Quantitative comparison of the phospho-histone 3 S-10 bands. Results produced from three independent experiments. **c** The confocal time-lapse images showing an example of a normal/unperturbed HeLa H2B-GFP cell undergoing the cell cycle in mitosis. **d** An example of a HeLa H2B-GFP cell undergoing apoptosis after prolonged mitotic arrest by 60 ng/ml nocodazole or 60 ng/ml nocodazole + 50 μM M2I-1. The white arrowhead indicates the time point when the cytoplasmic membrane (DIC grey images) of the cell starts shrinking and rounding up with condensed chromosomes (green). The diamond heads indicate the time point that the cytoplasmic membrane began blebbing. The chromosomes displaying fragmentation and over-condensation are highlighted by white dashed arrows and normal arrows respectively. A typical apoptotic-body like morphology is highlighted with the asterisk. **e** An example of a HeLa H2B-GFP cell undergoing apoptosis at a prophase-like stage induced by treatment with 60 ng/ml nocodazole + 50 μM M2I-1. The white arrowhead highlights the time point where there is clear cell body shrinkage, dash arrows highlight the fragmenting chromosomes and normal black arrows indicate the intact cytoplasmic membrane during chromosome fragmentation. Asterisks highlight the formation of a typical apoptotic-body like morphology. The green histone 2B-GFP highlights the chromosomal morphologies and the DIC images in grey indicate the cellular boundaries and the cytoplasmic membrane. The timing of the images is indicated

slippage, live images of a HeLa cell line over-expressing a Histone 2B-GFP fusion protein were recorded for 24 h using a Nikon A1R fully automated high-speed confocal imaging system under conditions described previously [6]. The Histone 2B-GFP signals were used to visualise the chromosomal morphology, which determines the cell cycle stage and chromosomal status; DIC images were used to reveal the morphological changes in the cytoplasmic membrane (Fig. 2c, normal cell cycle).

Cells were seen to round up with condensed chromosomes as they arrested at prometaphase-like states in response to the nocodazole treatment (Fig. 2d white arrowheads). The beginning of cell death was defined as a cell starting to show blebbing of its cytoplasmic membrane (Fig. 2d, diamond heads) or to display shrinkage of the cell body (Fig. 2e, black arrowheads). This was followed by the production of overcondensed chromosomes (Fig. 2d, e, white dash line arrows) or breaking of the chromosomes (Fig. 2d, e, white solid arrows), and the formation of a typical late stage apoptotic body (Fig. 2d, e, white asterisks) [34]. The slippage of a cell was determined by the decondensation of the prometaphase-like arrested chromosomes with no cytoplasmic division (Fig. 3a, arrows) and the regaining of their cytoplasmic membrane attachment (Fig. 3a, dash line arrows) [29].

The quantification of the mitotic and cell death indices using this histone 2B-GFP line (Fig. 3b, c) shows similar patterns to the previous observations (Fig. 1). There were significant increases in the cell death after 16 and 24 h of treatment with NOC + M2I-1 compared to nocodazole alone (Fig. 3b). In a separate experiment, we examined the mitotic index and apoptotic index at 24, 36 and 48 h (Fig. 3d, e). As expected the number of cells arrested in mitosis gradually reduced after 24 h (Fig. 3d), and this was correlated with the increased cell death (Fig. 3e), however, the amount of cell death induced by the presence of NOC + M2I-1 is significantly higher at each time point compared to that induced by nocodazole alone (Fig. 3e).

Given that M2I-1 induces the premature degradation of Cyclin B1 in the presence of nocodazole [6], then if the Cyclin B1 levels continue to decrease after prolonged mitotic arrest, more cells might undergo mitotic exit and escape mitotic cell death. Surprisingly though, slippage could rarely be identified in cells treated either with nocodazole alone or NOC + M2I-1 within the entire 24 h recording time, and whilst there was a slight increase in slippage events after 48 h of treatment, there were no significant differences observed between these two treatments (Fig. 3f). Instead, cell death was induced within the same cell cycle, and the majority of these cells begin to die after 16 h of mitotic arrest (Fig. 2d). Therefore, the reduced levels of histone H3 S-10 phosphorylation in samples treated with the NOC + M2I-1 compared to samples treated with nocodazole alone was a consequence of the reduced mitotic cell population caused by cell death (Figs. 1c, 2a, b). A small proportion (~5%) of these dead cells entered the cell death programme with a prophase-like morphology (Fig. 2e). These cells developed severe chromosomal degeneration or fragmentation first (Fig. 2e, dash line arrows) and displayed less blebbing of the cytoplasmic membrane (Fig. 2e black arrows). The typical apoptotic body-like morphology was only formed at a very late stage in the process (Fig. 2e white asterisk).

M2I-1 induced caspase-3 cleavage in the presence of nocodazole

As the majority of the cells that died after a prolonged arrest showed typical apoptotic morphology, we examined caspase-3 cleavage to confirm that the apoptotic pathway had contributed to their cell death. The results showed that the cleavage of caspase-3 remained very low or undetectable in both the control samples treated with 0.5% DMSO and the samples treated with 50 μM M2I-1

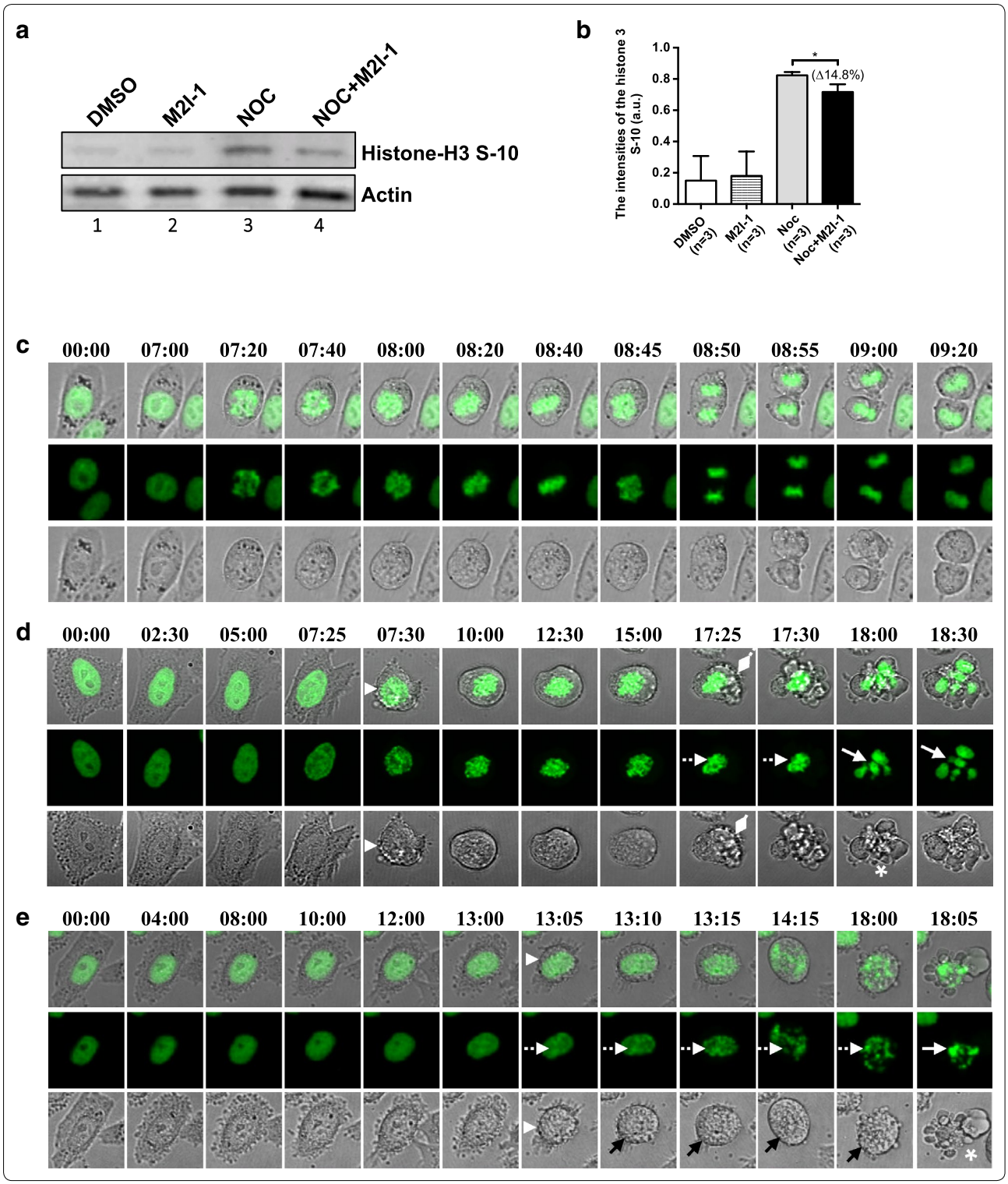

alone (Fig. 4a, lanes 1 and 2). Samples prepared from cells treated with 60 ng/ml of nocodazole alone showed some cleavage of caspase-3 (Fig. 4a, lane 3 and b), and the level from cells treated with NOC + M2I-1 was significantly higher (Fig. 4a, lane 4 and b). Thus, the cell death induced by M2I-1 in the presence of nocodazole is associated with the caspase-3 dependent apoptotic pathway.

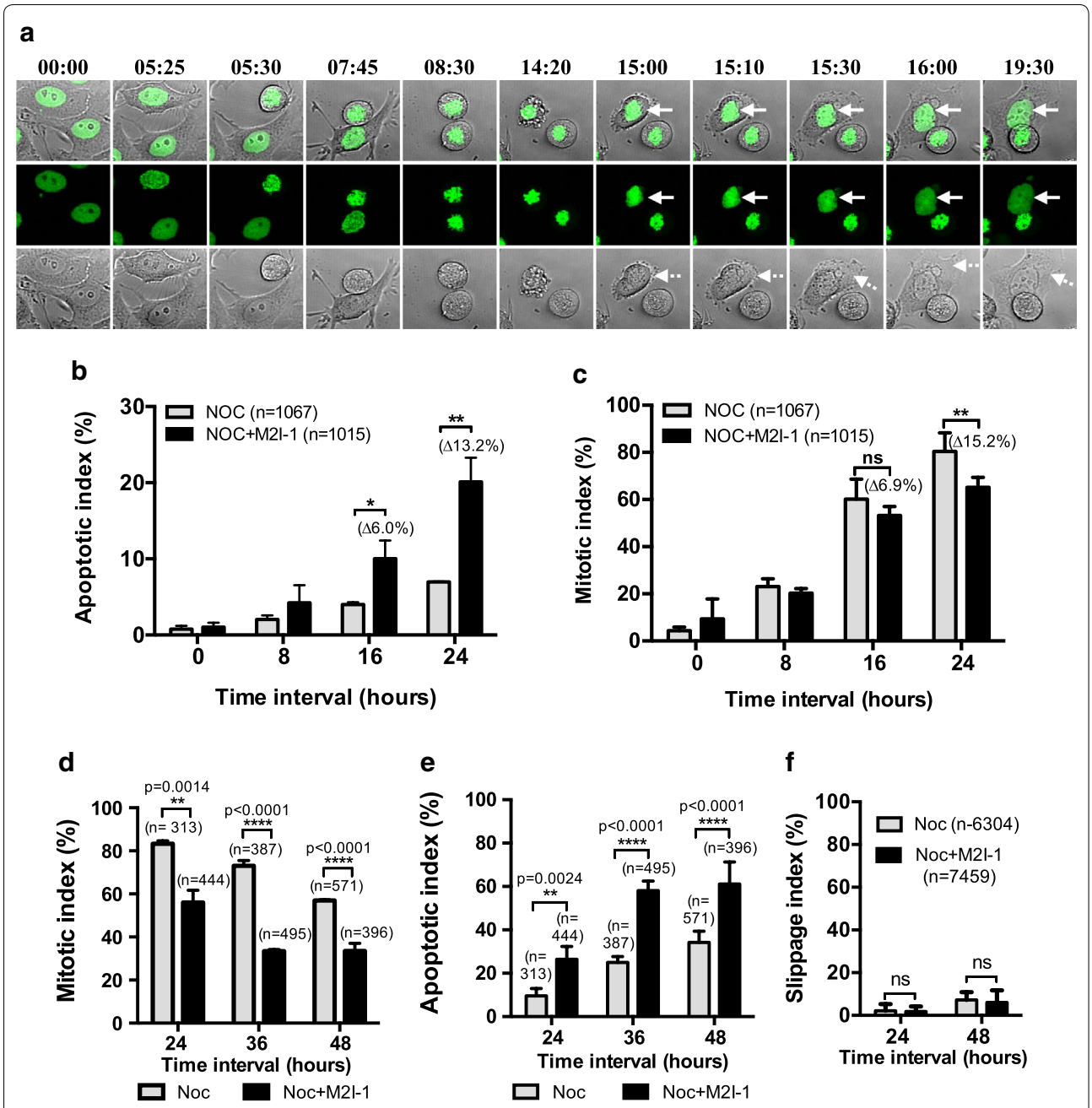

Fig. 3 The comparison of the amount of slippage and mitotic status of the HeLa cells caused by the various drug treatments. The cells used are the same cells as for Fig. 2. **a** An example of confocal time-lapse images showing a HeLa H2B-GFP cell undergoing slippage. The white arrows indicate the chromosomes that are undergoing premature decondensation without cytokinesis having taken place. The white dash line arrows highlight the re-attachment of the cytoplasmic membrane. **b** The quantitative cell death that occurred after prolonged mitotic arrest from cells treated with 60 ng/ml nocodazole alone (grey border) or 60 ng/ml nocodazole + 50 μM M2I-1 treatment (black border). The results were produced from three independent experiments. *P value: < 0.012, **P value < 0.002. **c** Quantitative results showing the mitotic indices due to the different drug treatments (color-coded as above) at different time intervals. **P value < 0.002. **d** Quantitative results showing the mitotic indices due to the different drug treatments (black/grey borders the same as above) at different time intervals as indicated. P values shown as indicated. **e** Quantitative results showing the apoptotic indices due to the different drug treatments (color-coded the same as above) at different time intervals as indicated. P values shown as indicated. **f** Quantitative results comparing the slippage rates between different drug treatments (color-coded same as above). The data from three independent experiments were used for the quantifications. n, cell numbers used for quantification; ns, not significant

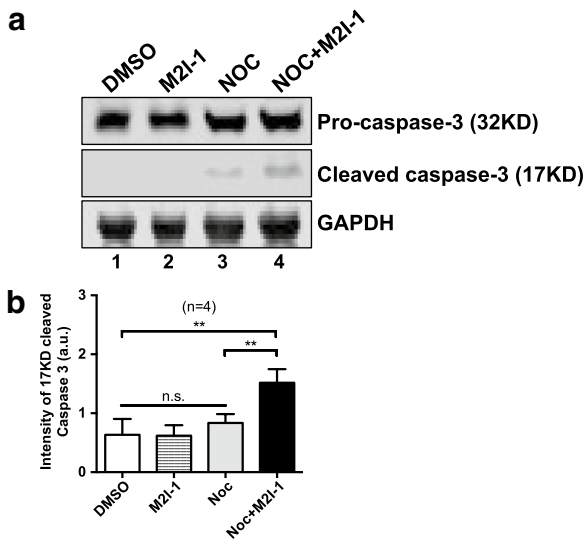

Fig. 4 M2I-1 induced caspase-3 activity in the presence of nocodazole. **a** Cell extracts were prepared from HeLa cells under different drug treatments as indicated. 60 µg/lane of total protein from each sample was loaded for protein separation using a 10% precast SDS-PAGE tris-bis protein gel, and after western blotting the membranes were probed with an anti-caspase-3 antibody (Abcam, ab32351, 1:1000 dilutions), an anti-GAPDH antibody (Thermo Fisher Scientific, MA5-15738, 1:1000 dilutions) which acted as the loading control. Lane 1: HeLa cells treated with 0.5%DMSO (v/v) as control; lane 2: Cells treated with 50 µM M2I-1; lane 3: Cells treated with 60 ng/ml nocodazole; and lane 4: Cells treated with 60 ng/ml nocodazole + 50 µM M2I-1 for 24 h. **b** Quantitative results comparing the cleaved form of the caspase-3 from western blots of three independent experiments. P value ** < 0.0026

The DNA damage checkpoint is less likely to contribute to this specific cell death

To examine if these cell deaths could be caused by DNA damage, we analysed the formation of γ-H2AX foci (a newly phosphorylated histone 2AX, H2A histone family member X), a typical indicator of DNA double-strand breaks [35] and used VP16 (etoposide) as a positive control as it is known to induce DNA damage [36]. The percentage of cells containing more than five γ-H2AX foci from un-arrested cells at the cell cycle stage similar to the cells treated with VP16, indicated by the morphology of their DAPI staining, has been used to represent the DNA damage level at each time point [37]. After 16 h of treatment with either NOC or NOC + M2I-1 there were insufficient numbers of un-arrested cells for quantification, so we have compared the average fluorescent intensities of the γ-H2AX foci from the mitotically arrested cells despite the fact that DNA-PKcs/CHK2 can also increase the level of γ-H2AX in mitotically arrested HeLa cells in the absence of DNA damage [37]. We anticipated that if there were additional DNA damage caused by the M2I-1 in the presence of nocodazole, we would see a higher level of γ-H2AX. The confocal images (Fig. 5a) and the quantitative results (Fig. 5b) showed that cells treated with nocodazole alone or NOC + M2I-1 have slightly more γ-H2AX foci compared to the DMSO negative control and this suggests that some DNA damage occurred under these two conditions. However, these levels of DNA damage were rather weak when compared to the levels seen in the positive control which was cells treated with VP16 for only 2 h (Fig. 5a, b). More importantly, there is no significant difference in this small amount of DNA damage at each time point examined. All of which suggests that the DNA damage pathway is not involved in the cell death induced by M2I-1 in the presence of nocodazole.

M2I-1 in the presence of nocodazole induced the down-regulation of Cyclin B1

Cyclin B1 is the regulatory subunit of Cdk1, and its level is regulated by the anaphase-promoting complex or cyclosome (APC/C) [2, 38]. Under certain circumstances Cyclin B1 has been regarded as an essential molecule in the determination of tumor cell fates [14, 34]. Previously it has been shown that targeting Cyclin B1 inhibits proliferation and sensitizes cancer cells to taxol [14, 15], and that apoptosis induced by drugs is often accompanied by the down-regulation of Cyclin B1 [14, 39]. To test if M2I-1 could prevent the accumulation of Cyclin B1, HeLa cells were treated as described before for 16 h and then fixed and antibody stained using the PLA method described previously [6] (Fig. 6a). The samples made from cells treated with M2I-1 showed significantly reduced amounts of Cyclin B1 in prophase or mitosis compared to control cells (Fig. 6a), and this was confirmed by the quantitative results (Fig. 6b). This premature Cyclin B1 degradation connected with a weakened SAC was confirmed by showing that M2I-1 disrupted the in vivo interaction between CDC20 and MAD2 in mitotic HeLa cells [6]. This was further supported by the observation of an overall reduction in Cyclin B1 detected by western blot (Fig. 8a lane 2 and 4).

The role of "competing-networks" cannot apply to the cell death induced by M2I-1 in the presence of nocodazole

MCL-1 (myeloid cell leukemia 1) is a pro-survival member of the Bcl-2 family of proteins [40]. It prevents the oligomerisation of the pro-apoptotic proteins Bak and Bax on the mitochondrial membrane, and so, stops the release of cytochrome C thus avoiding the activation of caspase [40, 41]. In unperturbed normal HeLa cells the expression of MCL-1 is cell cycle regulated, its levels increase during mitosis and peak around metaphase and early anaphase, but remained low in interphase

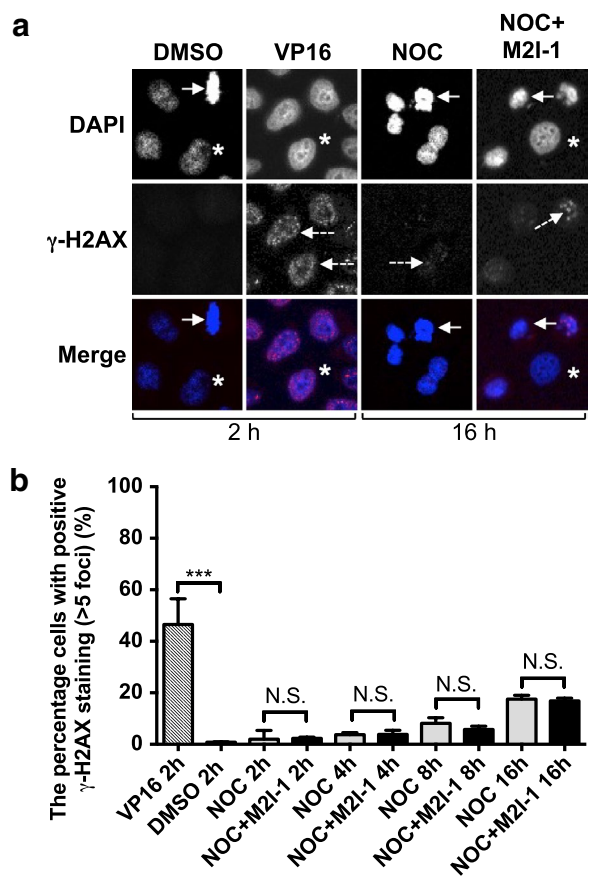

Fig. 5 The comparison of the γ-H2AX foci formation profiles under the different drug treatment conditions. **a** Representative confocal images showing the γ-H2AX foci formed in HeLa cells at different cell cycle stages. Arrows indicate a metaphase cell treated with 0.5% DMSO for 2 h (negative control), or a prometaphase-like cell from those treated with 60 ng/ml nocodazole (NOC) alone, and 60 ng/ml NOC + 50 μM M2I-1 for 16 h respectively. Cells treated with 10 mM VP16 for 2 h act as a positive control. Asterisks highlight those un-arrested cells after NOC and NOC + M2I-1 treatment or ones from the negative control at a similar cell cycle stage to the VP16 treated cells as justified by their DNA morphologies. These cells were fixed with 4% formamide-PBS solution and stained with a primary anti-γ-H2AX antibody (Abcam, ab-2893, 1:500 dilutions). The specific fluorescent signals of the γ-H2AX foci were illustrated by a Cy5 secondary antibody (Abcam, ab6564, 1:500 dilutions) in red and were indicated by dash line arrows. DNA was stained with DAPI and is shown in blue. **b** The quantitative results comparing the DNA damage levels indicated by the percentage of cells having more than 5 γ-H2AX foci from the cell population being treated at different time intervals as indicated. Under a 40x oil objective lens, the cells from four or five random areas of the confocal images were taken to give the quantitative results. Three independent experiments were conducted to produce the data. P value *** < 0.003. NS, not significant

(Fig. 7a). In response to the nocodazole provoked SAC it is degraded (Fig. 7b bottom panel) and that degradation can be prevented by MG132 (Fig. 7b bottom panel).

The degradation of MCL-1 is associated with the triggering of apoptosis in many different types of cells [42, 43] and its phosphorylation by Cyclin B1-dependent Cdk1 kinase facilitates this degradation [44]. It has been suggested that the accumulation of Cyclin B1 caused by an active SAC facilitates the degradation of MCL-1 to promote apoptosis, and vice versa [45]. A more recently proposed "competing-networks" model suggests that the rise of an as yet undefined death signal competes with the survival signal generated by the reduction of Cyclin B1 to determine whether the cell dies in mitosis or exits and returns to interphase [20, 34].

We, therefore, examined the protein profiles of Cyclin B1 and MCL-1 from the samples described above (Fig. 8a). As expected, when Cyclin B1 was stabilized by the treatment with nocodazole alone, it was associated with a significant reduction of MCL-1 (Fig. 8a, lane 3), and the lowered Cyclin B1 induced by the combined drugs, is associated with an elevated MCL-1 (Fig. 8a, lane 4). This is a surprise when the cell death observed previously (Fig. 1b, d) is also considered. The levels of the pro-apoptotic proteins BIM, BID, and PUMA remained relatively unchanged or even slightly reduced (Fig. 8b–d), but the level of NOXA increased marginally (Fig. 8f lane 4). However, the levels of an anti-survival protein, MCL-1s (a short form variant of the full-length MCL-1 which acts to sequester the function of MCL-1), increased when the cells were treated with NOC + M2I-1 compared to nocodazole alone (Fig. 8a lane 4 and e lane 4). Therefore, the increased levels of the pro-apoptotic proteins MCL-1s and NOXA might antagonize the increased level of MCL-1. In order to test this speculation, live-cell images were recorded examining the behaviour of a cell line (MCF-7) which lacks the expression of MCL-1s [46], in response to prolonged mitotic arrest in the presence of nocodazole and M2I-1 or nocodazole alone. The experiment was conducted using the same conditions as described in Fig. 2 apart from determination of the chromosomal morphologies which was illustrated by staining with 0.2 μM SiR-DNA (Tebu-Bio, UK) [47]. As with HeLa cells, the mitotic index began to reduce in the group treated with both drugs after 16 h of incubation, and this became significant at 20 h compared to the cells treated with nocodazole alone (Fig. 8g). However, in contrast to HeLa cells, M2I-1 failed to induce cell death in the presence of nocodazole in MCF-7 cells over the time course of the observations (Fig. 8h), and the reduced mitotic index in MCF-7 cells after double drug treatment is caused by cell slippage (Fig. 8i). As MCL-1s is a short form and the consequence of an alternative splicing event of the full length MCL-1 pre-mRNA [48, 49], it is impossible to design siRNA experiments

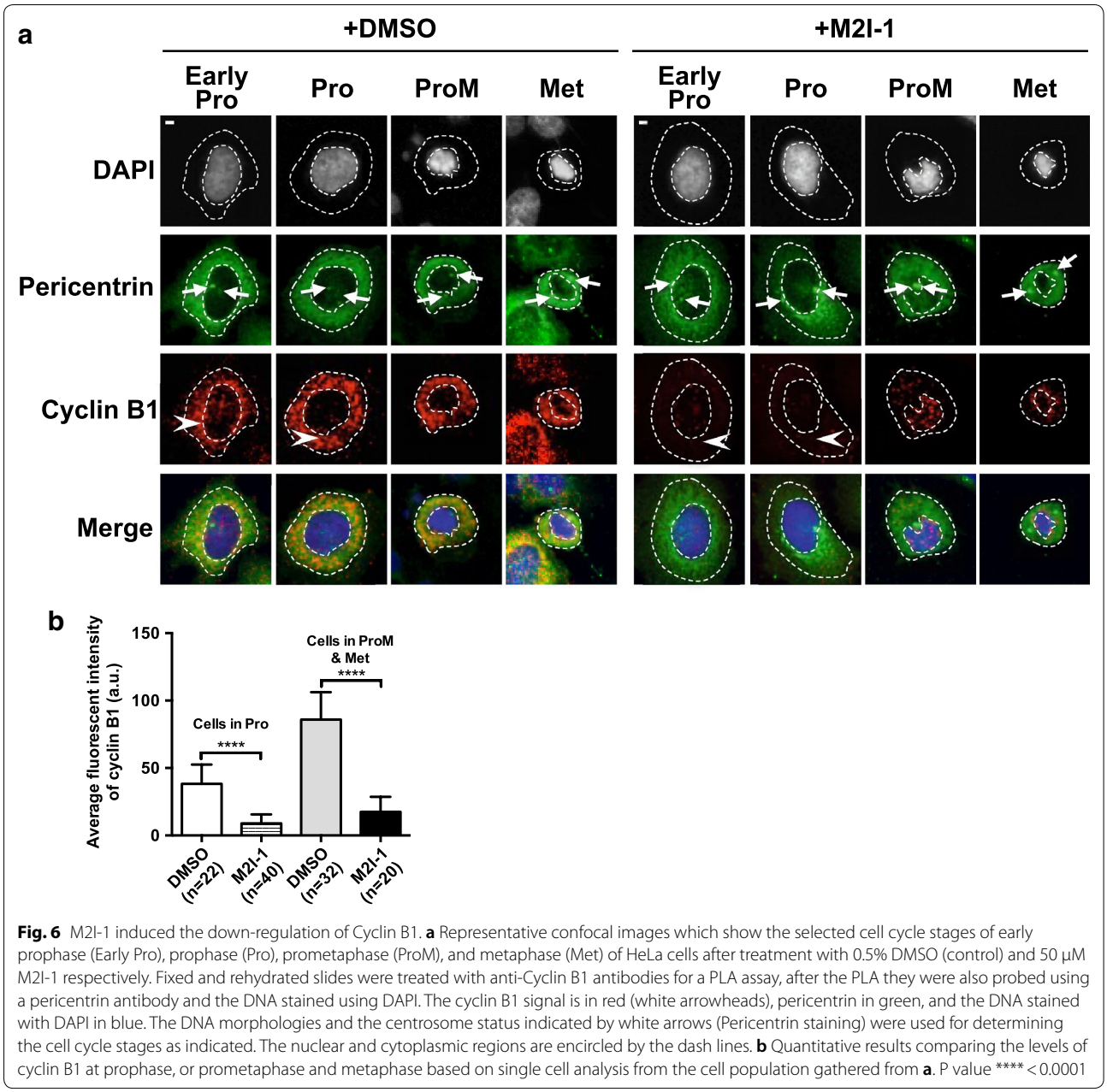

Fig. 6 M2I-1 induced the down-regulation of Cyclin B1. **a** Representative confocal images which show the selected cell cycle stages of early prophase (Early Pro), prophase (Pro), prometaphase (ProM), and metaphase (Met) of HeLa cells after treatment with 0.5% DMSO (control) and 50 μM M2I-1 respectively. Fixed and rehydrated slides were treated with anti-Cyclin B1 antibodies for a PLA assay, after the PLA they were also probed using a pericentrin antibody and the DNA stained using DAPI. The cyclin B1 signal is in red (white arrowheads), pericentrin in green, and the DNA stained with DAPI in blue. The DNA morphologies and the centrosome status indicated by white arrows (Pericentrin staining) were used for determining the cell cycle stages as indicated. The nuclear and cytoplasmic regions are encircled by the dash lines. **b** Quantitative results comparing the levels of cyclin B1 at prophase, or prometaphase and metaphase based on single cell analysis from the cell population gathered from **a**. P value **** < 0.0001

that directly and specifically target MCL-1s for depletion in HeLa cells, and so we transfected the MCF-7 cell line with the plasmid DNA of pCMV-AN-mGFP-MCL-1s so that it would express the exogenous GFP-MCL-1s protein. These transfected cells (Fig. 9, lane 3 and 4) along with the normal MCF-7 cells (Fig. 9, lane 1 and 2) were then treated with the drugs as described above, and the samples were prepared for western blot analysis. As MCF-7 cells also lack the expression of caspase-3 [50, 51], we examined the cleavage of PARP-1 (Poly [ADP-ribose] polymerase 1) to evaluate the apoptotic activity, as it is a well-established biomarker for cell death [52, 53]. The lack of expression of the endogenous MCL-1s in these samples (Fig. 9, lane 1–4), and the expression of the exogenous GFP-MCL-1s fusion protein in the transfected MCF-7 cells (Fig. 9, lane 3 and 4) were confirmed using a specific anti-MCL-1 antibody. The endogenous MCL-1 in these MCF-7 cells behaved the same as it had done in the HeLa cells. Its levels increased when cells were treated with the combined drugs NOC + M2I-1 compared to the cells treated with nocodazole alone (Fig. 9a, lanes 2

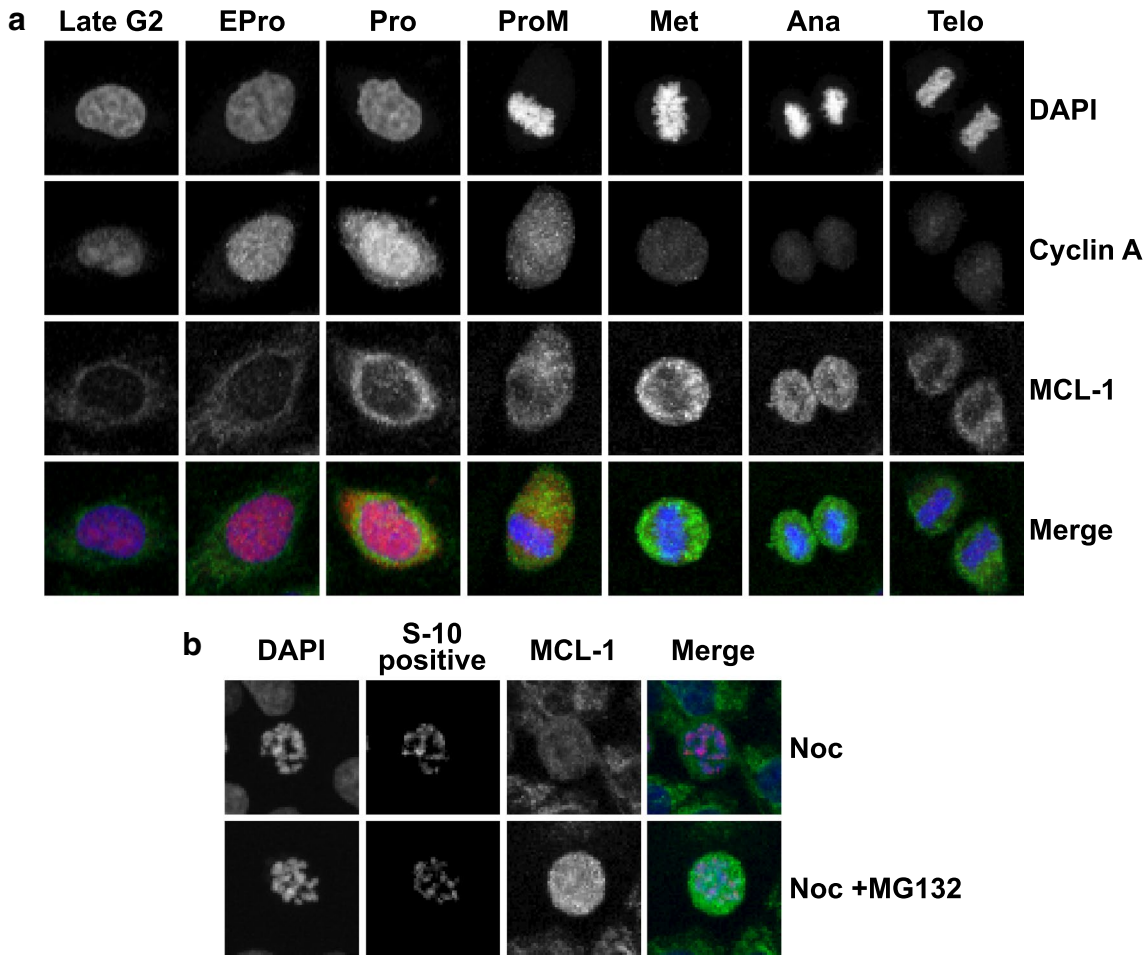

Fig. 7 The regulation of the stabilities of MCL-1, Cyclin A in HeLa cells. **a** Representative confocal images showing the expressions and distributions of the MCL-1 (green in merged images) in unperturbed HeLa cells at different cell cycle stages as indicated. Cyclin A in red (merged images, Santa Cruz, sc-271682, mouse monoclonal anti-cyclin A (B-8) 1:500 dilutions). These cells were fixed with 4% formamide-PBS solution and stained with a primary anti-Mcl-1 (S-19, Santa Cruz, sc-819) antibody (1:500 dilutions) or anti-Cyclin A (B-8) antibody (Santa Cruz, sc-271682) (1:500 dilutions). DNA was stained with DAPI (blue in merged images). The distributions of the fluorescent signals of Cyclin A throughout the cell cycle used for timing the cell cycle stages for comparison purpose. **b** Representative confocal images showing the expressions of MCL-1 (green) in nocodazole arrested (top panel) or nocodazole and MG132 arrested (bottom panel) HeLa cells. DNA was stained with DAPI (blue in merged images) and the mitotic status highlighted by staining with the phosphor-histone H3 S-10 antibody (red, Cell signalling, 9706, 1:200 dilutions). HeLa cells were treated with nocodazole or nocodazole + MG132 for 8 h

and 4 compared to lanes 1 and 3). Similarly, the level of exogenous GFP-MCL-1s is also increased in the sample treated with the combined drugs (Fig. 9a, lane 4 compared to lane 3). The results show that the level of the cleaved PARP-1 increased significantly in the sample treated with NOC + M2I-1 compared to the sample treated with nocodazole alone in the cells transfected with GFP-MCL-1s (Fig. 9a, lane 3 and 4 and b). In contrast, only very low levels of PARP-1 and no significant difference in its cleavage could be detected from the normal MCF-7 cells after treatment with the same conditions as above (Fig. 9a, lanes 1 and 2). Thus, MCL-1s is the main factor that antagonizes the elevated level of MCL-1 and causes the cell death induced by M2I-1 in the presence of nocodazole or taxol.

Discussion

M2I-1 (MAD2 inhibitor-1) is the first small molecule that has been identified which disrupts the CDC20-MAD2 interaction both in vitro and in vivo, an essential process in the assembly of the MCC [6, 27]. We have previously reported that M2I-1 can prevent the formation of the CDC20-MAD2 complex both at prophase before NEBD (nuclear envelope break-down) and at prometaphase and

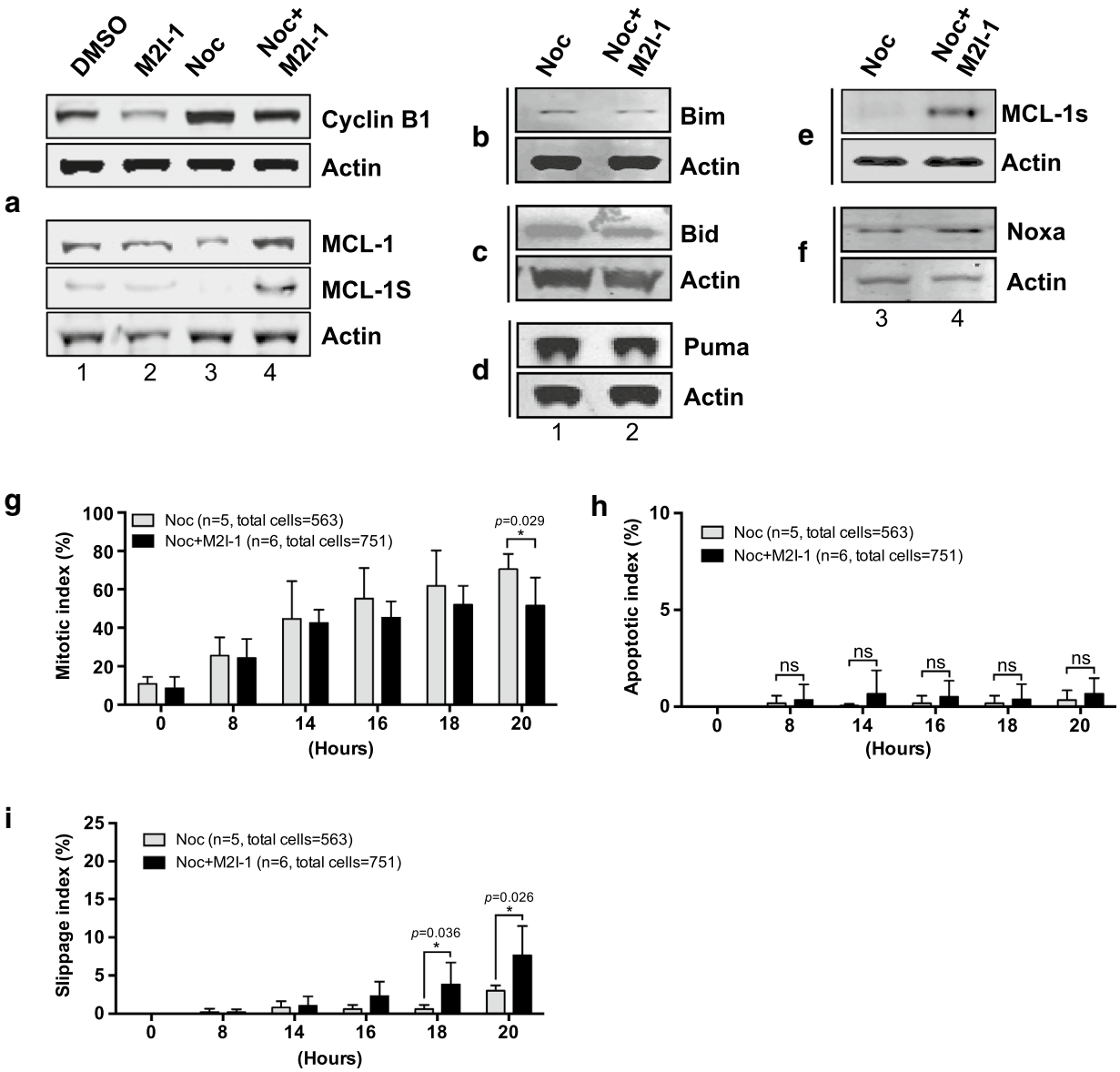

Fig. 8 The regulation of the stability of MCL-1, cyclin B1, and other pro- or anti-apoptotic proteins in HeLa and MCF-7 cells. **a** Western blots of cell extracts prepared from HeLa cells after treatment with 0.5% DMSO, 50 μM M2I-1, 60 ng/ml nocodazole, and 60 ng/ml nocodazole + 50 μM M2I-1 respectively and probed with a rabbit polyclonal anti-cyclin B1 antibody (H-433) antibody (sc-7520); a mouse monoclonal anti-actin (AC-15) antibody (ab6276) was used as the loading control. **b**–**f** Western blot results showing the expression levels of the pro-apoptotic proteins BIM, BID, PUMA, NOXA, and MCL-1s in HeLa cells. Cell extracts were prepared from HeLa cells after treatment with nocodazole alone or nocodazole + M2I-1 as described before. Actin bands were used as the loading controls. MCF-7 cells were treated using the same conditions as described in Fig. 2e apart from the determination of the chromosomal morphologies, which was highlighted by staining with 0.2 μ M SiR-DNA. Digital images were taken after 20 h incubation for quantification of the mitotic (**g**), apoptotic (**h**), and slippage indices (**i**). n: The number of the parallel experiments and the total cell numbers used for quantification. P value * < 0.026, 0.029, and 0.036 respectively

metaphase [6]. We have also found that the disruption of the interaction between CDC20 and MAD2 induced by the M2I-1 treatment correlated with the premature degradation of Cyclin B1 at both stages (Fig. 6a, b) [6]. Intriguingly, we show here that M2I-1 could significantly increase the sensitivity of several lines of cancer cells to anti-mitotic drugs such as nocodazole and taxol both within 24 h or beyond (Figs. 1, 3). It has been believed that when a cell is in a prolonged mitotic arrest, a gradually declining level of Cyclin B1 and a stabilised level of MCL-1serve as a survival signal which competes with an as yet undefined death signal to determine whether the

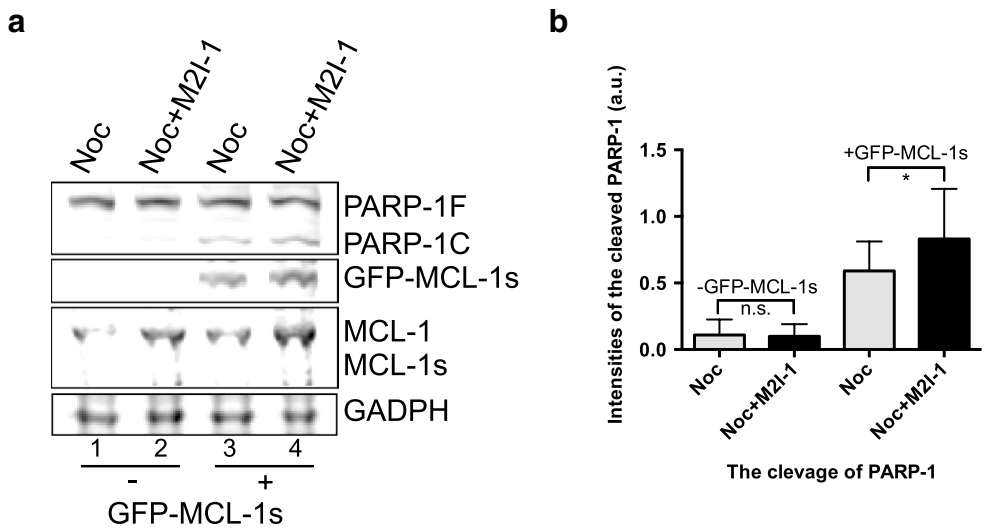

Fig. 9 Ectopically expressed mGFP-MCL-1s sensitizes the MCF-7 cells to M2I-1 in the presence of nocodazole. **a** Western blot results showing the expression levels of PARP-1F (full length) and its cleaved fragment PARP-1C, MCL-1, MCL-1s and the exogenous GFP-MCL-1s. GAPDH was used as the loading control. **b** The quantification of the cleaved PARP-1C under the experimental condition used in **a**. Data was quantified from three independent experiments after being normalised with the loading control. Paired *t* test. P value: * < 0.014

cell dies in mitosis or exits and returns to interphase [20, 34, 45]. Our results, however, suggest that in HeLa cells under the current experimental conditions, the accumulation of Cyclin B1 with a reduced MCL-1 would not trigger apoptosis; moreover, an elevated MCL-1 and lowered Cyclin B1 would not directly trigger slippage either (Figs. 1, 2, 3, 6, 8). More interestingly, M2I-1 in the presence of nocodazole or taxol could induce cell death in cells with a low level of Cyclin B1 and stabilized MCL-1 under a weakened SAC (Figs. 1, 3, 6, 8). This phenomenon cannot be explained by the "competing-networks" model [20]. Most likely, the premature degradation of Cyclin B1 caused by the M2I-1 treatment throughout the cell cycle combined with the microtubule network disruption caused by nocodazole or taxol reduced the cells fitness. The increased levels of the pro-apoptotic proteins MCL-1s and NOXA antagonized the pro-survival function of MCL-1 and triggered cells into undergoing apoptosis (Figs. 8, 9).

Conclusion

We have shown that as a single agent M2I-1 cannot cause cancer cell death, but it can significantly increase many cancer cells sensitivity to anti-mitotic drugs, such as nocodazole and taxol within the same cell cycle. This might prove to be significant, as it would increase the clinical efficacies of current drugs such as taxanes, epothilones, and vinca alkaloids and potentially reduce the length of treatment as well as the dose used. It might also slow any developing resistances and the possibility of relapse or new tumorigenesis after chemotherapy using current anti-mitotic drugs, though this has yet to be tested. We have also discovered some important molecular mechanisms for understanding the relationships between the mitotic checkpoint and programmed cell death.

Materials and methods

Antibodies and reagents

Primary antibodies used in this project are Rabbit polyclonal anti-CDC20 antibody (Abcam, ab26483); mouse monoclonal anti-p55 CDC (E-7) (Santa Cruz Biotech, sc-13162); rabbit polyclonal anti-full length MAD2 (Convance, PRB-452C); mouse monoclonal anti-cyclin B1 (GNS) (Santa Cruz, sc-245); mouse monoclonal anti-cyclin A (B-8) (Santa Cruz, sc-271682); mouse monoclonal anti-actin antibody (Abcam, ab6276); mouse monoclonal anti-GADPH antibody (Thermo Fisher Scientific, MA5-15738); rabbit polyclonal anti-caspase-3 antibody (Abcam, ab32351); rabbit polyclonal anti-phospho-histone 3 (S-10) antibody (Millipore, #06-570); and rabbit polyclonal anti-GFP antibody [Santa Cruz, sc-8334 (GP-FL)]; rabbit polyclonal anti-γ-H2AX (S-139) antibody (Abcam, ab-2893); GFP-Trap A geta-20 (ChromoTek, 70112001A); rabbit polyclonal anti-Mcl-1 (S-19) antibody (Santa Cruz, sc-819); rabbit polyclonal anti-pericentrin 1&2 antibody (Abcam, ab4448); rabbit polyclonal anti-BID (FL-195) antibody (Santa Cruz, sc-11423); mouse monoclonal anti-BIM (H-5) antibody (Santa Cruz, sc-374358); rabbit polyclonal anti-NOXA (FL-54) antibody (Santa Cruz, sc-30209) and monoclonal

anti-PUMA (G-3) antibody (Santa Cruz, sc-374223); rabbit monoclonal anti-human PARP-1 antibody (46D11) (Cell Signaling Technology).

Secondary antibodies goat polyclonal secondary antibody to rabbit IgG-H + L (DyLight 488) (Abcam, ab96899), goat anti-rabbit polyclonal IgG-H&L (Cy5), pre-adsorbed (Abcam, ab6564), IRDye 680 donkey anti-mouse (926–322227; LI-COR Biosciences), and IRDye 800CW donkey anti-mouse (926–32212; LI-COR Biosciences).

Duolink reagents Duolink In Situ PLA probe anti-Rabbit PLUS, Duolink In Situ PLA probe anti-Mouse Minus, Duolink In Situ Detection Reagents Red (the Duolink assay reagent kits are distributed by Sigma-Aldrich).

Chemicals M2I-1 (ChemBridge Corporation), CelLytic™ MT Cell Lysis Reagent (Sigma-Aldrich, C3228), Protease inhibitor cocktail (Sigma-Aldrich, p8340), Thymidine (Sigma-Aldrich, Cas-358801), Nocodazole (Sigma-Aldrich, Cas-31430-18-9), Taxol (Paclitaxel, T7402) (Sigma-Aldrich), VP16 (etoposide) (Sigma-Aldrich, E1383), DMEM (Sigma-Aldrich), DAPI (4′, 6-Diamidine-2′-phenylindole dihydrochloride) (Sigma-Aldrich, D9542), DMSO (Dimethylsulfoxide, Santa Cruz, sc-358801). Odyssey blocking solution (Li_Cor Biosciences UK Ltd). SiR-DNA and Verapamil (Tebu-Bio).

Plasmid DNA and cell transfection

The original pcDNA3-flag-MCL-1s (human) was kindly provided as a gift by Professor Jeehyeon Bae's lab at Chung-ANG university of South Korea. The plasmid DNA was used as a template for PCR (polymerase chain reaction) to generate the MCL-1s DNA fragment incorporated with Sgf1 and Mul1 restriction enzyme sites at its 5′ and 3′ ends respectively. This PCR fragment of Sgf1-MCL-1(s)-Mul1 was subsequently subcloned into a mammalian expression vector, pCMV6-AN-mGFP, at Sgf1 and Mul1 sites, in frame with and downstream of the mGFP sequence. The primer pair used for MCL-1s PCR, was 5′ forward: GAATTCGCGATCGCCATGTTTGGC CTCAAAAGAAACGC and 3′ reverse: GAATTCACG CGTTCACAGTAAGGCTATCTTATTAGATATGC.

The plasmid DNA transfections were performed using the LipofectamineTM3000 kit (ThermoFisher Scientific, UK) according to the commercial protocol. Briefly, MCF-7 cells were grown in a T75 flask with 14 ml of an antibiotic-free DMEM medium up to 70% confluence. 1 μg/ml of pCMV6-AN-mGFP-MCL-1s plasmid DNA was used for transfection. The solution containing the DNA lipid complex was added to MCF-7 cells for incubation at 37 °C supplied with 5% CO_2 for 24 h. The transfected cells were harvested and resuspended in 12 ml of fresh complete medium and were split equally and seeded into 6 wells of a 6-well plate. The cells were used for drug treatment after all of them attached to the wells, which normally took about 6–8 h.

Cell culture conditions and treatments

The HeLa cell line overexpressing histone 2B-GFP, A549, HT29, U2OS and the RPE1CCNB1-Venus cells (a gift from Jonathan Pines' lab, RPE1, a human retinal pigment epithelial cell line) was cultured in DMEM medium (Dulbecco's Modified Eagle Medium) as described before [6]. Cells were treated with 30 nM Taxol [34], 10 μM VP16, and 60 ng/ml (equivalent to 200 nM) nocodazole [5] or with 50 μM M2I-1 [27], or M2I-1 and nocodazole together in 0.5% DMSO for the lengths of time discussed in the results. Subsequently the treated or untreated HeLa cells were fixed using 1 ml cold (−20 °C) methanol [8] and left at room temperature for 5 min, or were fixed with 1 ml of 4% formamide-PBS (phosphate-buffer saline) solution for 10 min at room temperature and then stored at −20 °C for later use. Cell extracts prepared using the same drug treatments but with increased culture volumes were used for western blotting.

Protein gel and western blotting

The cell extracts for gel electrophoresis, and western blotting were prepared as described before [6]. Cells were lysed in an appropriate amount of CelLytic™ MT Cell Lysis Reagent containing 1 × protease inhibitor cocktail on ice with agitation for 30 min. Samples of the cell lysates were separated using a precast 10% Bis–Tris SDS-PAGE gel (sodium dodecyl sulfate polyacrylamide gel electrophoresis), and were then transferred onto a nitrocellulose membrane for western blotting. The membranes were blocked in 1x Odyssey blocking solution for 1 h and then probed with appropriate primary antibodies in Odyssey blocking solution (1:500 dilution) at room temperature for 2 h or at 4 °C overnight with agitation. The membrane was then incubated with a secondary antibody solution of IRDye 680 donkey anti-mouse, or IRDye 800CW donkey anti-mouse, at 1:2000 dilutions for one and a half hours. The fluorescence signals were detected using a CCD scanner (Odyssey; LI-COR Biosciences) according to the manufacturer's instructions.

Immunofluoresence for γ-H2AX

HeLa cells on a coverslip prepared as described above were washed three times in 1× PBS, and blocked with a blocking solution of 5% BSA (bovine serum albumin) in 1xPBS for an hour at room temperature followed by incubation with a primary mouse anti-human γ-H2AX antibody at a dilution of 1:500 in blocking solution. The cells were incubated overnight at 4 °C. Cells were washed twice in 1× PBS and once with 1× PBST (1× PBS + 0.1% Tween-20), for 5 min each. This was followed

by incubation with a Cy5 goat anti-mouse IgG secondary antibody at a dilution of 1:500 in blocking solution containing an appropriate amount of DAPI at room temperature for 90 min in the dark. After being washed twice in 1× PBS, and once with 1× PBST and air-dried as above the cells on the coverslips were mounted with an appropriate amount of 50% glycerol-PBS solution and sealed using nail vanish for later use.

PLA fluorescent immunostaining

The Duolink based proximity ligation assay (PLA) was conducted as described previously [6] with the following changes. The paired primary antibodies used were a mouse monoclonal anti-Cyclin B1 and a rabbit polyclonal anti-Cyclin B1 (H-433).

Confocal imaging and quantification of the fluorescent complexes

The stained HeLa cells were scanned using a Leica TCS SP2 laser scanning confocal system same as described before [6].

The live images of the histone 2B-GFP in HeLa cells or MCF-7 cells stained with 0.2 μM SiR-DNA to illustrate the chromosome morphologies were recorded using a Nikon A1R fully automated high-speed confocal imaging system with a time interval of 5 min over 24 h.

ImageJ, Photoshop, and NIS-elements were used for quantification, editing of the fluorescent intensities of the complex or live imaging processing where appropriate.

Abbreviations

M2I-1: MAD2 inhibitor-1; MCC: mitotic checkpoint complex; APC/C: anaphase-promoting complex or cyclosome; SAC: spindle assembly or mitotic checkpoint; NOC: nocodazole; H2AX: H2A histone family member X; VP16: etoposide; DMSO: dimethylsulfoxide; MCL-1: myeloid cell leukemia 1; PARP-1: poly [ADP-ribose] polymerase 1; NEBD: nuclear envelope break-down; PLA: proximity ligation assay; PCR: polymerase chain reaction; RPE1: a human retinal pigment epithelial cell line; DMEM: Dulbecco's modified eagle medium; SDS-PAGE: sodium dodecyl sulfate polyacrylamide gel electrophoresis; BSA: bovine serum albumin; PBS: phosphate-buffer saline.

Acknowledgements

We thank Dr. Yan Zhao (NICR Newcastle University) for providing the HT-29, A549, U2OS and MCF-7 cell lines. We also thank Prof. John Higgins and Dr. Diana Papini for the HeLa H2B-GFP cell line. We thank Dr. Ian Cowell (ICaMB, Newcastle University) for the γH2AX antibody and VP16 and Prof. Jeehyeon Bae (School of Pharmacy, Chung-ANG Univ. Republic Korea) for the pCDNA3-MCL-1L and MCL-1S plasmid DNA constructs. We particularly thank Mr. Michael Aitchison for critical editorial comments.

Author's contributions

J-YH designed, performed, and analysed the experiments and wrote the manuscript. JQL contributed to Figs. 1, 2, 3, 4, 5, 6 and 8; NMD contributed to Figs. 2, 3, 5, 8 and 9; NML contributed to Fig. 4; PAJ contributed to Figs. 8 and 9; DH contributed to Fig. 7; FG and RNL contributed to Fig. 4. All authors read and approved the final manuscript.

Funding

J. Li, N. Dang and J-Y. Huang: were supported by Ph.D. fees; N.M-L: was funded by the Rosetrees Trust and the Stoneygate Trust, internal funds from Newcastle University, and an Early Researcher Award from Newcastle University Institute for Ageing (BH154239); P.J.: was funded from National Institute for Health Research Health Protection Research Unit (NIHR HPRU) in Chemical & Radiation Threats & Hazards at Newcastle University (HPRU-2012-10076); R. L. & F. G.: were funded from Wellcome Trust programme Grant [096919].

Availability of data and materials

All data generated or analyzed in this study are included in the article.

Ethics approval and consent to participate

Not applicable.

Consent for publication

All authors have read and agreed to the final version of the manuscript.

Competing interests

The authors declare that they have no competing interests.

Author details

[1] Institute for Cell and Molecular Biosciences, Newcastle University, Framlington Place, Newcastle upon Tyne NE2 4HH, UK. [2] Medical Toxicology Centre, Institute of Cellular Medicine, NIHR Health Protection Research Unit, Newcastle University, Claremont Place, Newcastle upon Tyne NE1 4AA, UK. [3] Present Address: Intensive Care Unit, Guizhou Provincial People's Hospital, Guiyang, People's Republic of China. [4] Present Address: Department of Pediatric Critical Care Medicine, Guizhou Provincial People's Hospital, Guiyang, People's Republic of China.

Received: 6 March 2019 Accepted: 5 June 2019
Published online: 15 June 2019

References

1. Rieder CL, Cole RW, Khodjakov A, Sluder G. The checkpoint delaying anaphase in response to chromosome monoorientation is mediated by an inhibitory signal produced by unattached kinetochores. J Cell Biol. 1995;130(4):941–8.
2. Lara-Gonzalez P, Westhorpe FG, Taylor SS. The spindle assembly checkpoint. Curr Biol. 2012;22(22):R966–80.
3. Musacchio A, Salmon ED. The spindle-assembly checkpoint in space and time. Nat Rev Mol Cell Biol. 2007;8(5):379–93.
4. Li X, Nicklas RB. Mitotic forces control a cell-cycle checkpoint. Nature. 1995;373(6515):630–2.
5. Sudakin V, Chan GK, Yen TJ. Checkpoint inhibition of the APC/C in HeLa cells is mediated by a complex of BUBR1, BUB3, CDC20, and MAD2. J Cell Biol. 2001;154(5):925–36.
6. Li J, Dang N, Wood DJ, Huang JY. The kinetochore-dependent and -independent formation of the CDC20-MAD2 complex and its functions in HeLa cells. Scientific Rep. 2017;7:41072.
7. Clute P, Pines J. Temporal and spatial control of cyclin B1 destruction in metaphase. Nat Cell Biol. 1999;1(2):82–7.
8. Huang J, Raff JW. The disappearance of cyclin B at the end of mitosis is regulated spatially in Drosophila cells. EMBO J. 1999;18(8):2184–95.
9. Yu H. Structural activation of Mad2 in the mitotic spindle checkpoint: the two-state Mad2 model versus the Mad2 template model. J Cell Biol. 2006;173(2):153–7.
10. Chao WC, Kulkarni K, Zhang Z, Kong EH, Barford D. Structure of the mitotic checkpoint complex. Nature. 2012;484(7393):208–13.
11. Liu ST, Zhang H. The mitotic checkpoint complex (MCC): looking back and forth after 15 years. AIMS Mol Sci. 2016;3(4):597–634.
12. Poddar A, Stukenberg PT, Burke DJ. Two complexes of spindle checkpoint proteins containing Cdc20 and Mad2 assemble during mitosis independently of the kinetochore in *Saccharomyces cerevisiae*. Eukaryot Cell. 2005;4(5):867–78.
13. Rodriguez-Bravo V, Maciejowski J, Corona J, Buch HK, Collin P, Kanemaki MT, Shah JV, Jallepalli PV. Nuclear pores protect genome integrity by assembling a premitotic and Mad1-dependent anaphase inhibitor. Cell. 2014;156(5):1017–31.

14. Androic I, Kramer A, Yan R, Rodel F, Gatje R, Kaufmann M, Strebhardt K, Yuan J. Targeting cyclin B1 inhibits proliferation and sensitizes breast cancer cells to taxol. BMC Cancer. 2008;8:391.
15. Yuan J, Yan R, Kramer A, Eckerdt F, Roller M, Kaufmann M, Strebhardt K. Cyclin B1 depletion inhibits proliferation and induces apoptosis in human tumor cells. Oncogene. 2004;23(34):5843–52.
16. Chen RH. BubR1 is essential for kinetochore localization of other spindle checkpoint proteins and its phosphorylation requires Mad1. J Cell Biol. 2002;158(3):487–96.
17. Orth JD, Loewer A, Lahav G, Mitchison TJ. Prolonged mitotic arrest triggers partial activation of apoptosis, resulting in DNA damage and p53 induction. Mol Biol Cell. 2012;23(4):567–76.
18. Burgess A, Rasouli M, Rogers S. Stressing mitosis to death. Front Oncol. 2014;4:140.
19. Bakhoum SF, Silkworth WT, Nardi IK, Nicholson JM, Compton DA, Cimini D. The mitotic origin of chromosomal instability. Curr Biol. 2014;24(4):R148–9.
20. Gascoigne KE, Taylor SS. How do anti-mitotic drugs kill cancer cells? J Cell Sci. 2009;122(Pt 15):2579–85.
21. Janssen A, Kops GJ, Medema RH. Targeting the mitotic checkpoint to kill tumor cells. Horm Cancer. 2011;2(2):113–6.
22. de Carcer G, Perez de Castro I, Malumbres M. Targeting cell cycle kinases for cancer therapy. Curr Med Chem. 2007;14(9):969–85.
23. Salmela AL, Kallio MJ. Mitosis as an anti-cancer drug target. Chromosoma. 2013;122(5):431–49.
24. McGrogan BT, Gilmartin B, Carney DN, McCann A. Taxanes, microtubules and chemoresistant breast cancer. Biochim Biophys Acta. 2008;1785(2):96–132.
25. Schmidt M, Bastians H. Mitotic drug targets and the development of novel anti-mitotic anticancer drugs. Drug Resist Updates. 2007;10(4–5):162–81.
26. Komlodi-Pasztor E, Sackett D, Wilkerson J, Fojo T. Mitosis is not a key target of microtubule agents in patient tumors. Nat Rev Clin Oncol. 2011;8(4):244–50.
27. Kastl J, Braun J, Prestel A, Moller HM, Huhn T, Mayer TU. Mad2 inhibitor-1 (M2I-1): a small molecule protein–protein interaction inhibitor targeting the mitotic spindle assembly checkpoint. ACS Chem Biol. 2015;10:1661.
28. Hahn AT, Jones JT, Meyer T. Quantitative analysis of cell cycle phase durations and PC12 differentiation using fluorescent biosensors. Cell Cycle. 2009;8(7):1044–52.
29. Rieder CL, Maiato H. Stuck in division or passing through: what happens when cells cannot satisfy the spindle assembly checkpoint. Dev Cell. 2004;7(5):637–51.
30. Harper JV. Synchronization of cell populations in G1/S and G2/M phases of the cell cycle. Methods Mol Biol. 2005;296:157–66.
31. Matsui Y, Nakayama Y, Okamoto M, Fukumoto Y, Yamaguchi N. Enrichment of cell populations in metaphase, anaphase, and telophase by synchronization using nocodazole and blebbistatin: a novel method suitable for examining dynamic changes in proteins during mitotic progression. Eur J Cell Biol. 2012;91(5):413–9.
32. Goldstein JC, Kluck RM, Green DR. A single cell analysis of apoptosis. Ordering the apoptotic phenotype. Ann New York Acad Sci. 2000;926:132–41.
33. Ziegler U, Groscurth P. Morphological features of cell death. News Physiol Sci. 2004;19:124–8.
34. Gascoigne KE, Taylor SS. Cancer cells display profound intra- and interline variation following prolonged exposure to antimitotic drugs. Cancer Cell. 2008;14(2):111–22.
35. Khanna KK, Jackson SP. DNA double-strand breaks: signaling, repair and the cancer connection. Nat Genet. 2001;27(3):247–54.
36. Duca M, Guianvarc'h D, Oussedik K, Halby L, Garbesi A, Dauzonne D, Monneret C, Osheroff N, Giovannangeli C, Arimondo PB. Molecular basis of the targeting of topoisomerase II-mediated DNA cleavage by VP16 derivatives conjugated to triplex-forming oligonucleotides. Nucleic Acids Res. 2006;34(6):1900–11.
37. Tu WZ, Li B, Huang B, Wang Y, Liu XD, Guan H, Zhang SM, Tang Y, Rang WQ, Zhou PK. gammaH2AX foci formation in the absence of DNA damage: mitotic H2AX phosphorylation is mediated by the DNA-PKcs/CHK2 pathway. FEBS Lett. 2013;587(21):3437–43.
38. Sivakumar S, Gorbsky GJ. Spatiotemporal regulation of the anaphase-promoting complex in mitosis. Nat Rev Mol Cell Biol. 2015;16(2):82–94.
39. Castedo M, Perfettini JL, Roumier T, Yakushijin K, Horne D, Medema R, Kroemer G. The cell cycle checkpoint kinase Chk2 is a negative regulator of mitotic catastrophe. Oncogene. 2004;23(25):4353–61.
40. Kozopas KM, Yang T, Buchan HL, Zhou P, Craig RW. MCL1, a gene expressed in programmed myeloid cell differentiation, has sequence similarity to BCL2. Proc Natl Acad Sci USA. 1993;90(8):3516–20.
41. Thomas LW, Lam C, Edwards SW. Mcl-1; the molecular regulation of protein function. FEBS Lett. 2010;584(14):2981–9.
42. Nijhawan D, Fang M, Traer E, Zhong Q, Gao W, Du F, Wang X. Elimination of Mcl-1 is required for the initiation of apoptosis following ultraviolet irradiation. Genes Dev. 2003;17(12):1475–86.
43. Zhong Q, Gao W, Du F, Wang X. Mule/ARF-BP1, a BH3-only E3 ubiquitin ligase, catalyzes the polyubiquitination of Mcl-1 and regulates apoptosis. Cell. 2005;121(7):1085–95.
44. Kobayashi S, Lee SH, Meng XW, Mott JL, Bronk SF, Werneburg NW, Craig RW, Kaufmann SH, Gores GJ. Serine 64 phosphorylation enhances the antiapoptotic function of Mcl-1. J Biol Chem. 2007;282(25):18407–17.
45. Mocciaro A, Rape M. Emerging regulatory mechanisms in ubiquitin-dependent cell cycle control. J Cell Sci. 2012;125(Pt 2):255–63.
46. Gautrey HL, Tyson-Capper AJ. Regulation of Mcl-1 by SRSF1 and SRSF5 in cancer cells. PLoS ONE. 2012;7(12):e51497.
47. Lukinavicius G, Blaukopf C, Pershagen E, Schena A, Reymond L, Derivery E, Gonzalez-Gaitan M, D'Este E, Hell SW, Gerlich DW, et al. SiR-hoechst is a far-red DNA stain for live-cell nanoscopy. Nat Commun. 2015;6:8497.
48. Bae J, Leo CP, Hsu SY, Hsueh AJ. MCL-1S, a splicing variant of the antiapoptotic BCL-2 family member MCL-1, encodes a proapoptotic protein possessing only the BH3 domain. J Biol Chem. 2000;275(33):25255–61.
49. Bingle CD, Craig RW, Swales BM, Singleton V, Zhou P, Whyte MK. Exon skipping in Mcl-1 results in a bcl-2 homology domain 3 only gene product that promotes cell death. J Biol Chem. 2000;275(29):22136–46.
50. Kurokawa H, Nishio K, Fukumoto H, Tomonari A, Suzuki T, Saijo N. Alteration of caspase-3 (CPP32/Yama/apopain) in wild-type MCF-7, breast cancer cells. Oncol Rep. 1999;6(1):33–7.
51. Janicke RU. MCF-7 breast carcinoma cells do not express caspase-3. Breast Cancer Res Treat. 2009;117(1):219–21.
52. Kaufmann SH, Desnoyers S, Ottaviano Y, Davidson NE, Poirier GG. Specific proteolytic cleavage of poly(ADP-ribose) polymerase: an early marker of chemotherapy-induced apoptosis. Can Res. 1993;53(17):3976–85.
53. Chaitanya GV, Steven AJ, Babu PP. PARP-1 cleavage fragments: signatures of cell-death proteases in neurodegeneration. Cell Commun Signal. 2010;8:31.

Publisher's Note

Springer Nature remains neutral with regard to jurisdictional claims in published maps and institutional affiliations.